Performance Evaluation of Blind Tropospheric Delay correction Models over Africa

^{1,2,} Olalekan Adekunle Isioye, ^{2,1}Ludwig Combrinck, ³Joel Botai

DOI: http://dx.doi.org/10.4314/sajg.v4i4.10

Abstract

Tropospheric delay is a major error source in positioning by Global Navigation Satellite Systems (GNSS). Many techniques are available for tropospheric delay mitigation consisting of surface meteorological models and global empirical models. Surface meteorological models need surface meteorological data to give high accuracy mitigation while the global empirical models need not. However, most GNSS stations in the African region are not equipped with a meteorological sensor for the collection of surface meteorological data during the measurement. Zenith Tropospheric Delay (ZTD) is often calculated by the various high precision GNSS software packages by utilising standard atmosphere values. Lately, researchers in the University of New Brunswick and Vienna University of Technology have both developed global models (University of New Brunswick (UNB3M) and Global Pressure and Temperature 2 wet (GPT2w) models) for tropospheric delay correction, respectively. This report represents an appraisal of the performance of the GPT2w and UNB3M models with accurate International GNSS Service (IGS)-tropospheric estimations for fifteen IGS stations over a period of 1 year on the Africa continent. Both models perform significantly better at low latitudes than higher latitudes. There was better agreement between the GPT2w model and the IGS estimate than the UNB3m at all stations. Thus, the GPT2w model is recommended as a correction model of the tropospheric error for the GNSS positioning and navigation on the African Continent.

Keywords: Global Navigation Satellite Systems (GNSS), Zenith Tropospheric Delay (ZTD), Zenith Wet Delay (ZWD), Zenith Hydrostatic Delay (ZHD), International GNSS Service (IGS), Blind Tropospheric models

¹ Department of Geography, Geoinformatics and Meteorology, University of Pretoria, Pretoria 0002, South Africa, u13390742@tuks.co.za

²Hartebeesthoek Radio Astronomy Observatory (HartRAO), P. O. Box 443, Krugersdorp 1740, South Africa, isioye@hartrao.ac.za

³South African Weather Service, 442 Rigel Avenue South, Erasmusrand, Pretoria 0001, South Africa

1.0 Introduction and background

Tropospheric delay is one of the main error sources in the analysis of space geodetic techniques operating at microwave frequencies, such as Global Navigation Satellite Systems (GNSS), Very Long Baseline Interferometry (VLBI), or Doppler Orbitography and Radiopositioning Integrated by Satellite (DORIS).

The tropospheric delay is usually separated into a hydrostatic delay that is modelled a priori, and a wet delay that is estimated from the space geodetic microwave observations. Modelled hydrostatic delays and the estimated wet delays are usually referred to the zenith direction; corresponding mapping functions are required to convert the slant delays in observation direction to the zenith. In addition, troposphere gradients can be estimated to account for asymmetries of the troposphere.

In GNSS positioning, the tropospheric delay typically ranges between 2.0 m to 2.6 m. The Zenith Hydrostatic Delay (ZHD) constitutes 90% of the Zenith Tropospheric Delay (ZTD), and Zenith Wet Delay (ZWD) is usually less than 10%. The ZHD can be estimated to an accuracy of better than 90% using empirical models that utilizes meteorological data, such as pressure and temperature as well as the position of the user. Some ZHD models include those of *Saastamoinen* (1972), *Hopfield* (1969), *Berman* (1976), *Davis et al* (1985), *Ifadis*(1986), *Askne and Nordius* (1987) etc. A comprehensive review and validations of some of these model can be found *in Tuka and El-Mowafy*(2013). The Saastamoinen model is the most used model in geodetic applications and its accuracy has been widely reported (*Dodo and Idowu*, 2010).

In practice, a user often employs a certain troposphere model based on the popularity of the model without giving enough justification as to why it should be used. Limited comparisons between some of the models have been carried out in the past for local or regional applications. However, in this contribution, this issue is addressed more comprehensively considering the peculiarities of the African GNSS network. Most GNSS stations on the African continent are characterised by the lack of collocated meteorological sensors, as it is required for such to be collocated with the GNSS antenna if the GNSS data are to be processed for integrated water vapour content determination (*Isioye et al., 2015*). Thus, the inversion of ground meteorological data into the variable vapour content in the atmosphere is very difficult. Even the Saastamoinen model has difficulties in meeting the needs for high accuracy GNSS positioning and meteorological applications, since most

GNSS geodetic software uses the Saastamoinen model with standard atmosphere models for a-poiri estimates.

In view of these shortcomings, it is of practical importance to construct a global model of average tropospheric delay correction with a certain accuracy to be used particularly in the GNSS navigation and positioning in Africa, in which the zenith delay depends only on the latitude, elevation of observing station, and the date of observation. Recently, several of these blind models have been developed such as the University of New Brunswick model; UNB3 (*Collins and Langley, 1999*), RTCA- Minimum Operational Performance Standards; MOPS (*RCTA, 2001*); European Geostationary Navigation Overlay Service; EGNOS (*Dodson et al., 1999; Penna et al., 2001*); UNB3m (where m stands for "modified") (*Leandro et al., 2006*); European Space Agency; ESA model (*ESA Galileo Programme, 2012*); Global Pressure Temperature 2; GPT2 (*Lagler et al., 2013*); and Global Pressure Temperature 2 wet; GPT2w (*Boehm et al., 2014*). Table 1 provides an overview of the different blind models.

Table 1: Overview of Blind Tropospheric Correction Models

	RTCA MOPS model	UNB3m model	ESA model	GPT2 model	GPT2w model	
Temporal Resolution	Annual	Annual	Daily + Annual	Annual + Semi annual	Annual + Semi annual	
Spatial Resolution	15°	15°	1.5°	5°	1°	
Source of climatological dataset	U.S. standard atmospheric supplements, 1966 (COESA, 1966)	U.S. standard atmospheric supplements, 1966 (COESA, 1966)	Numerical Weather Prediction model - ERA 15	Numerical Weather Prediction model - ERA Interim	Numerical Weather Prediction model - ERA Interim	
ZHD model	Saastamoinen (1972)	Davis et al,,	Saastamoinen (1972)	Saastamoinen (1972)	Saastamoinen (1972)	
ZWD model	Askne and Nordius (1987)	Davis et al,, 1985	Askne and Nordius (1987)	Saastamoinen (1972)	Askne and Nordius (1987)	
Mapping	Black and	Neill Mapping	Neill Mapping	Global	Vienna Mapping	

function	Eisner Mapping Function (Neill,		Function (Neill,	Mapping	function(Boehm et
	Function (Black	1996)	1996)	Function	al., 2006a)
	and Eisner,			(Boehm et al.,	
	1984)			2006b)	

It is evident from Table1 that the models can be classified into two groups, one based on a set of tabulated climatological data and the other from Numerical Weather Prediction (NWP) models. In the first category, the UNB3m is a refined version of UNB3 model (*Leandro et al.*, 2006) and thus superior to RTCA MOPS, which is the same as the UNB3 model except for the replacement of the Neill mapping function with the Black and Eisner model(*Leandro et al.*, 2006). Considering the other set of models, which are dependent on NWP data, theGPT2w model looks quite outstanding going by the spatial resolution of the model and also for the fact that the Vienna Mapping function is known to model tropospheric delay better that the Neil mapping function adopted by the ESA model (see, *Won et al.*, 2010; *Zus et al.*, 2015).

This paper presents an assessment of the UNB3m and GPT2w tropospheric models. The Zenith tropospheric estimations were compared from both models with the International GNSS Service (IGS) estimates. The study utilized the new IGS ZTD product (available at http://cddis.gsfc.nasa.gov/gps/products/trop_new) for the interval January 2013 to December 2013 and for 15 sites distributed on the African continent as indicated by the squares in Figure 1. The new IGS ZTD product is based on the precise point positioning (PPP) technique. It has a higher sampling rate and lower formal errors than the legacy IGS ZTD product and can be obtained with typical formal errors of 1.5–5 mm from the IGS (*Byun and Bar-Sever*, 2009). Gaps are common in the data, but at least 3 month of ZTD estimates are available for each site. The IGS data are down sampled from 5 minute to daily intervals. Detailed method of analysis and inferences are presented in the following sections of this paper.

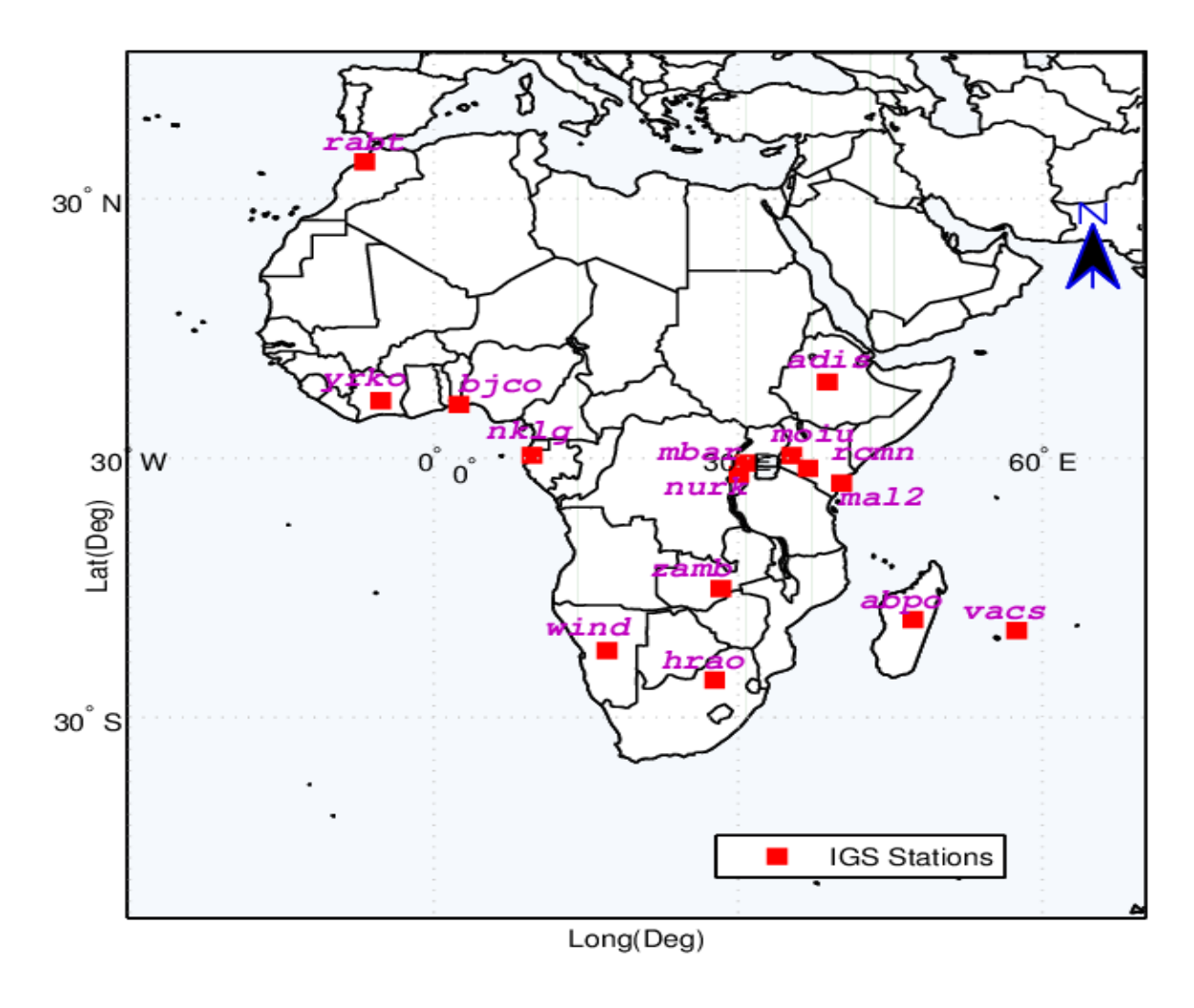


Figure 1: Map depicting the location of IGS stations in Africa

2.0 Description of tropospheric correction models adopted in this study

2.1 Saastamoinen model

Saastamoinen (1972) applied the gas laws to refractivity by considering the atmosphere as a mixture of dry air and water vapour. The model considers the temperature in the troposphere as decreasing with increasing height at a uniform rate, which varies slightly with latitude and season. However, in the polar region, there is a permanent inversion in the lower troposphere where the actual temperature increases with height. Saastamoinen assumed the neutral atmosphere to consist of two layers: the polytropic troposphere, which extends from the earth's surface to an altitude of approximately 11-12 km and the stratosphere, which is an isothermal layer, extending to approximately 50 km. The atmospheric water vapour is confined in the region of the troposphere only.

The Saastamoinen model for ZHD, in metres, is expressed as:

$$ZHD = 0.002277 \cdot \frac{P}{1 - 0.00266\cos(2\phi) - 0.28 \cdot 10^{-6} h}$$
 [1]

In Equation (1), P is the surface pressure in mbar, ϕ is latitude in radians and, h is the height of the surface above the ellipsoid (in metres).

In the zenith wet delay model, *Saastamoinen* (1972) assumed that there is a linear decrease of temperature with height, and that the water vapour pressure decreases with height. The variation of the water vapour pressure e_s (*mbar*) is expressed by the following expression:

$$e_{s} = RH \times 6.11 \times 10^{\frac{7.5T_{s}}{T_{s} + 273.15}}$$
 [2]

In Equation (2), RH is the relative humidity to be determined from local observations, and the surface temperature in Kelvin is T_s .

Saastamoinen (1972) gave the expression for the zenith wet delay model using the refractivity constant of Essen and Froome (1951) and for mid-latitudes and average conditions:

$$ZWD = 0.002277 \left(\frac{1255}{T_s} + 0.05 \right) e_s$$
 [3]

2.2 UNB3m Hydrostatic Delay Model

Leandro et al. (2006) presented a hybrid neutral atmosphere model designed for radiometric space users. This model, called UNB3m, has its algorithm based on the prediction of meteorological parameter values, which are then used to compute hydrostatic and non-hydrostatic zenith delays using the Saastamoinen model.

In order to account for the seasonal variation of the neutral atmosphere behaviour, a look-up table of meteorological parameters is used. The parameters are barometric pressure, temperature, water vapour pressure (WVP), temperature lapse rate (β) and water vapour pressure height factor (λ) . This look-up table was derived from the U.S. Standard Atmosphere Supplements, 1966 (*COESA*, 1966; Orliac, 2002). Table (2) lists the look-up table values for UNB3m. The data are divided into two groups, to account for the annual average (mean) and amplitude of a cosine function for each parameter. Both amplitudes and averages vary with respect to latitude, for all parameters. In the development of the UNB3m model, water vapour pressure in an earlier version of UNB3 was replaced with relative

humidity values in Table (2). This addressed the problem of overestimation of humidity in the UNB3 model. In UNB3m, all computations for the point of interest are done initially using relative humidity, which is subsequently converted to water vapour pressure for use in the zenith delay computation. The conversion is done in line with the conventions of the International Earth Rotation and Reference Frame Services (IERS) (*McCarthy &Petit*, 2004; *Leandro et al.*, 2006). Further details about the earlier model's (UNB3) development and performance are contained in *Collins and Langley* (1997, 1998).

Table 2: Look-up table of meteorological parameters for the UNB3m model, the parameters are user latitude zone (ϕ) barometric pressure (P_{\circ}) , temperature (T_{\circ}) , Relative Humidity (RH), temperature lapse rate (β) and water vapour pressure height or decrease factor (λ) (modified after Leandro et al., 2006)

Average									
$\varphi_{\text{(deg)}}$	$P_o[hPa]$	$T_o[K]$	RH(%)	$\beta_o[K/m]$	λ[-]				
15	1013.25	299.65	75.0	0.00630	2.77				
30	1017.25	294.15	80.0	0.00605	3.15				
45	1015.75	283.15	76.0	0.00558	2.57				
60	1011.75	272.15	77.5	0.00539	1.81				
75	1013.00	263.65	82.5	0.00453	1.55				
		Am	plitude						
$\varphi_{(\text{deg})}$	$\varphi_{ ext{(deg)}} \mid P_o[hPa] \mid T_o[K] \mid RH(\%) \mid \beta_o[K/m] \mid \lambda[-]$								
15	0.00	0.00	0.00	0.00000	0.00				
30	-3.75	7.00	0.0	0.00025	0.33				
45	-2.25	11.00	-1.0	0.00032	0.46				
60	-1.75	15.00	-2.5	0.00081	0.74				
75	-0.50	14.50	2.5	0.00062	0.30				

The first step in the UNB3m algorithm is to obtain the meteorological parameter values for a particular latitude and day of year using the look-up table. By definition, the origin of the yearly variation is day of year (doy) 28. This procedure is similar to the one used in the computation of the Niell mapping functions. The interpolation between latitudes is done with a linear function. The annual average of a given parameter can be computed as:

$$Avg_{\phi} = \begin{cases} Avg_{15}, & \text{if } \phi \leq 15 \\ Avg_{75}, & \text{if } \phi \geq 75 \\ Avg_{i} + \frac{\left(Avg_{i+1} - Avg_{i}\right)}{15} \left(\phi - Lat_{i}\right), & \text{if } 15 < \phi < 75 \end{cases}$$
[4]

In Equation (4) ϕ stands for the latitude of interest in degrees, Avg_{ϕ} is the computed average, i is the index of the nearest lower tabled latitude and Lat is their latitude (from Table 2). The annual amplitude can be computed in a similar manner:

$$Amp_{\phi} = \begin{cases} Amp_{15}, & \text{if } \phi \le 15 \\ Amp_{75}, & \text{if } \phi \ge 75 \\ Amp_{i} + \frac{\left(Amp_{i+1} - Amp_{i}\right)}{15} \left(\phi - Lat_{i}\right), & \text{if } 15 < \phi < 75 \end{cases}$$
[5]

In Equation (5) Amp_{ϕ} is the computed amplitude. After average and amplitude are computed for given latitude, the parameter values can be estimated for the desired day of year according to:

$$X_{\phi,doy} = Avg_{\phi} - Amp_{\phi} \cos\left((doy - 28)\frac{2\pi}{365.25}\right)$$
 [6]

where, $X_{\phi,doy}$ represents the computed parameter value for latitude ϕ and day of year (doy). This procedure is followed for each one of the three needed parameters. Once all parameters are determined for given latitude and day of year, the zenith hydrostatic delay can be computed according to:

$$ZHD = \frac{10^{-6} k_1 R}{g_m} \cdot P_o \cdot \left(1 - \frac{\beta H}{T_o}\right)^{\frac{g}{R\beta}}$$
 [7]

where, T_{\circ} , P_{\circ} , and β are meteorological parameters computed according to (4), (5), and (6); H is the orthometric height in metres; $k_1 = 77.60 \, Kmbar^{-1}$; R is the gas constant for dry air $\left(287.054 \, Jkg^{-1}K^{-1}\right)$; g is the surface acceleration of gravity in ms^{-2} ; g_m is the acceleration of gravity at the atmospheric column centroid in ms^{-2} and can be computed from:

$$g_m = 9.784 (1 - 2.66 \times 10^{-3} \cos(2\phi) - 2.8 \times 10^{-7} H)$$
 [8]

Leandro et al. (2006) presented the wet tropospheric refractivity for the station on the Earth's surface as a function of predicted meteorological parameter values. The model is analogous to the hydrostatic component and is expressed as (Farah, 2011):

$$ZWD = \frac{10^{-6} (T_{m} k_{2}' + k_{3}) R}{g_{m} \lambda' - \beta R} \frac{e_{o}}{T_{o}} \left(1 - \frac{\beta H}{T_{o}} \right)^{\left(\frac{\lambda' g}{R \beta} \right) - 1}$$
 [9]

In equation (9) T_{\circ} , $e_{\circ} \lambda$, P_{\circ} , and β are meteorological parameters computed according to equations (4-6); $k'_2 = 16.60 Kmbar^{-1}$; $\lambda' = \lambda + 1$ (unitless); T_m is the mean temperature of water vapour in Kelvin and can be computed from:

$$T_{m} = \left(T_{\circ} - \beta H\right) \left(1 - \frac{\beta R}{g_{m} \lambda'}\right)$$
 [10]

2.3 Global Pressure Temperature wet (GPT2w) Model

GPT2w is an extension of GPT and GPT2 (Boehm et al., 2007; Lagler et al., 2013) with improved capability to determine zenith delays in blind mode. The tropospheric model GPT2 itself is an enhancement of the Global Pressure and Temperature model (GPT; Boehm et al. 2007) and the Global Mapping Function (GMF; Boehm et al., 2006b). The development and validation of GPT2 as well as the comparison with GPT/GMF have been described in detail by Lagler et al. (2013). In its current version the ZHD and ZWD are a function of air pressure, temperature, water vapour pressure, latitude, and ellipsoidal height. The internally derived parameters (pressure, temperature, temperature lapse rate, water vapour pressure, hydrostatic and wet mapping function coefficients) are obtained from the statistical analysis of monthly mean ERA-Interim (European Centre For Medium- Range Weather Forecasts Re-Analysis) profiles over the time period 2001 to 2010. The mean values (A_s) as well as annual (A_1, B_1) and semi-annual amplitudes (A_2, B_2) for selected parameter r are computed as in Equation (11) and are stored as average value as well as amplitude of annual and semi-annual variations on a global grid with a resolution of 5° x 5° at mean ETOPO5 (Earth topography) height.

$$r(t) = A_0 + A_1 \cos\left(\frac{doy}{365.25} 2\pi\right) + B_1 \sin\left(\frac{doy}{365.25} 2\pi\right) + A_2 \cos\left(\frac{doy}{365.25} 4\pi\right) + B_2 \cos\left(\frac{doy}{365.25} 4\pi\right)$$
[11]

The parameters of Equation (11) are estimated at the four grid points surrounding the target location before extrapolating the parameters vertically to the desired height and interpolating the data from those base points to the observational site in the horizontal direction. The extrapolation of the hydrostatic mapping function follows *Niell* (1996),

whereas the wet mapping function is assumed to be constant in the vicinity of the Earth surface. The extrapolation of the pressure relies on an exponential trend coefficient related to the inverse of the virtual temperature, and the linear extrapolation of the temperature utilizes the GPT2 inherent temperature lapse rate. Surface grids for specific humidity within the GPT2 model have been derived from linear interpolation between pressure levels in the vicinity of Earth's surface. These parameters are used to determine values of zenith wet delays, by using the expressions of *Saastamoinen* (1972), although this approach is not optimal, it represents the starting point for the improved version of it. Thus, the GPT2w as an extension to GPT2 comes with an improved capability to determine zenith wet delays in blind mode (*Boehm et al.*, 2014; *Moller et al.*, 2013; *Schingelegger et al.*, 2014). The Saastamoinen formula was replaced with *Askne and Nordius* (1987) in the GPT2w model as reflected in Equation (12).

$$ZWD = 10^{-6} \left(k_2' + \frac{k_3}{T_m} \right) \frac{R_d}{(\lambda + 1) g_m} e_s$$
 [12]

In Equation (12), k'_2 and k_3 are refractivity constants, R_d is the specific gas constant for the dry component, g_m is the gravity acceleration at the centre of mass of the vertical atmospheric column and e_s is the water vapour pressure at the site.

Additionally, the GPT2w blind troposphere delay model provides the mean values plus annual and semi - annual amplitudes of pressure, temperature and its lapse rate, water vapour pressure and its decrease factor λ , weighted mean temperature, as well as hydrostatic and wet mapping function coefficients of the VMF1 (Vienna Mapping Function1). It also benefits from an improved spatial resolution of 1° .

All climatological parameters have been derived consistently from monthly mean pressure level data of ERA-Interim fields with a horizontal resolution of one degree, and the model is suitable to calculate slant hydrostatic and wet delays down to three degrees elevation at sites in the vicinity of the Earth surface using the date and approximate station coordinates as input.

3.0 Assessment of the accuracies of the UNB3m and GPT2w Models

The accuracies of the UNB3m and GPT2w models were evaluated using the new IGS ZTD product for the interval January 2013 to December 2013 and for 15 sites distributed on

the African continent. A summary of the individual station information is presented in Table 3.

Table 3: Station Information for selected IGS stations in Africa

Station	Country	Latitude(deg)	Longitude (deg)	Ellipsoidal Height
ABPO	Madagascar	-19.02	47.23	1552.99
ADIS	Ethiopia	9.04	38.77	2439.15
BJCO	Benin Republic	6.38	2.45	30.60
HRAO	South Africa	-25.89	27.69	1414.30
MAL2	Kenya	-3.00	40.19	-20.40
MBAR	Uganda	-0.60	30.74	1337.65
MOIU	Kenya	0.29	35.29	2201.53
NKLG	Gabon	0.35	9.67	31.48
NURK	Rwanda	-1.94	30.09	1485.30
RABT	Morocco	34.00	-6.85	90.10
RCMN	Kenya	-1.22	36.89	1607.54
VACS	Mauritius	-20.30	57.49	420.40
WIND	Namibia	-22.57	17.09	1734.70
YKRO	Cote d'Ivoire	6.87	-5.24	270.00
ZAMB	Zambia	-15.43	28.31	1324.91

The following performance indicators were adopted for the evaluation: Normalised Mean Absolute Error (NMAE) (Shcherbakov et al., 2013), Root Mean Square Error (RMSE), Model Efficiency (MEF) (Murphy, 1988), Reliability Index (RI) (Leggett and Williams, 1981), and Correlation coefficient (r). They performance indicators are represented as follows;

$$NMAE = \frac{\sum_{i=1}^{N} (|Bias_i|)}{N\overline{O}}$$

$$RMSE = \sqrt{\frac{\sum_{i=1}^{N} (Bias_i)^2}{N}}$$
[13]

$$RMSE = \sqrt{\frac{\sum_{i=1}^{N} (Bias_i)^2}{N}}$$
 [14]

$$MEF = 1 - \frac{\sum_{i=1}^{N} (Bias_i)^2}{\sum_{i=1}^{N} (|(P_i - \bar{O})| - |(O_i - \bar{O})|)^2}$$
[15]

$$RI = \exp\sqrt{\frac{1}{N} \sum_{i=1}^{N} \left(\log \frac{O_i}{P_i}\right)^2}$$
 [16]

$$r = \frac{\sum_{i=1}^{N} (P_i - \overline{P})(O_i - \overline{O})}{\left[\sum_{i=1}^{N} (P_i - \overline{P})^2 \cdot \sum_{i=1}^{N} (O_i - \overline{O})^2\right]^{1/2}}$$
[17]

In Equations (13) – (17), N is the number of observations, O_i and P_i are the " i^{th} " observed and model estimated values, \overline{O} and \overline{P} are the mean observed (IGS estimates) and model (UNB3m and GPT2w) estimated values, respectively, and $Bias_i = P_i - O_i$. A summary of the results of the different performance evaluator is presented in Table 4.

Table 4: Performance of the UNB3m and GPT2w for ZTD estimation against the IGS solutions

	NMAE	RMSE	MEF	RI	NMAE	RMSE	MEF	RI	NMAE	RMSE	MEF	RI
	ABPO		ADIS			BJCO						
GPT2w	0.0134	31.0320	0.8350	1.0152	0.0095	22.4626	0.8277	1.0123	0.0085	29.5480	0.7997	1.0115
UNB3M	0.0194	45.1071	0.3519	1.0223	0.0173	36.3694	0.3798	1.0199	0.0150	45.4024	0.4138	1.0176
		HRAO				MA	L2			MBA	4R	
GPT2w	0.0114	30.9544	0.8617	1.0149	0.0110	34.5622	0.6444	1.0135	0.0092	24.6734	0.5230	1.0115
UNB3M	0.0159	39.0528	0.6419	1.0189	0.0142	43.6633	0.3361	1.0171	0.0161	40.5798	0.4471	1.0190
		MO	IU			NKI	LG		NURK			
GPT2w	0.0092	26.0287	0.4370	1.0136	0.0069	22.7098	0.3916	1.0087	0.0100	26.4390	0.6495	1.0126
UNB3M	0.0154	34.8988	0.4482	1.0184	0.0193	55.4938	0.4100	1.0215	0.0170	42.3982	0.4510	1.0202
		RAI	BT			RCN	RCMN VACS					
GPT2w	0.0126	37.8190	0.5758	1.0157	0.0133	33.1069	0.4855	1.0160	0.0143	44.2097	0.7774	1.0185
UNB3M	0.0217	63.9707	0.4605	1.0265	0.0147	38.1572	0.4522	1.0185	0.0211	57.0262	0.5229	1.0242
		WIND		YKRO			ZAN	1B				
GPT2w	0.0140	35.3518	0.7838	1.0180	0.0080	26.2248	0.6363	1.0105	0.0132	33.1040	0.9013	1.0158
UNB3M	0.0218	48.4544	0.5628	1.0248	0.0158	44.7696	0.4170	1.0179	0.0302	70.1788	0.4344	1.0338

The NMAE measures the absolute deviation of the simulated values (UNB3m and GPT2w) from the observations (IGS estimates), normalised to the mean; a value of zero indicates perfect agreement and greater than zero an average fraction of the discrepancy normalised to the mean, the NMAE value from all the stations are indicative of the good performance of the GPT2w model. Similarly, RMSE measures the average square error with values near zero indicating a close match, the GPT2w model has a minimum RMSE of 22.4626 mm at ADIS and a maximum of RMSE of 44.2097 mm at VACS while for the UNB3m model, a maximum RMSE occur at ZAMB with a value of 70.1788 mm and minimum RMSE of 34.8988 mm at MOIU, thus, again the GPT2w performs better at all the stations. The MEF, which is a measure of the square of the deviation of the model's values (UNB3m and GPT2w) from the observations (IGS), normalised to the standard deviation of

the observed data (IGS values). MEF values range from [0, 1] as agreement between predicted values and observations change from no agreement (MEF = 0) to perfect agreement (MEF = 1). From Table 4 it is evident that the GPT2w model performs better at the stations with a range of 0.9013 to 0.3916, except at NKLG where a value of 0.3916 was obtained, the UNB3m model had a range of 0.6419 to 0.3361 which is indicative of a lower variability in the MEF compared to the GPT2w. The RI quantifies the average factor by which the model estimates differ from the IGS solutions. For example, an RI of 2 indicates that a model predicts the observations within a multiplicative factor of two, on average. Ideally, the RI should be close to one. When the RMSE is calculated for log transformed values of the predictions and observations, the RI is the exponentiated RMSE. The RI value for the two models under consideration is indicative of the strength of both models to predict ZTD within an acceptable average factor.

The time series plot of the UNB3m model, the GPT2w model, and the reference model (IGS) is shown in Figure 2. The ZTD estimated from GNSS as provided by the IGS show excellent diurnal characteristics, as the daily variations are very noticeable. However, the UNB3m and GPT2w models do not give good account for the daily variation in the ZTD estimates, but does provide a good estimate of the average daily variation across all the stations. The presence of the semi-annual amplitudes in the ZTDs is also evident in the plot of the GPT2w model across all the stations. Very prominent in the IGS, UNB3m and GPT2w time series is the annual cycle of the ZTD. Furthermore, the time series and Absolute Mean Difference (Error) (MAE) of the difference between each model and the IGS solution is presented in Figures 3(a) and (b). From both Figures, it is clear that the difference in ZTD estimate between the GPT2w and the IGS estimates is smaller than that of the UNB3m and the IGS estimates at all stations.

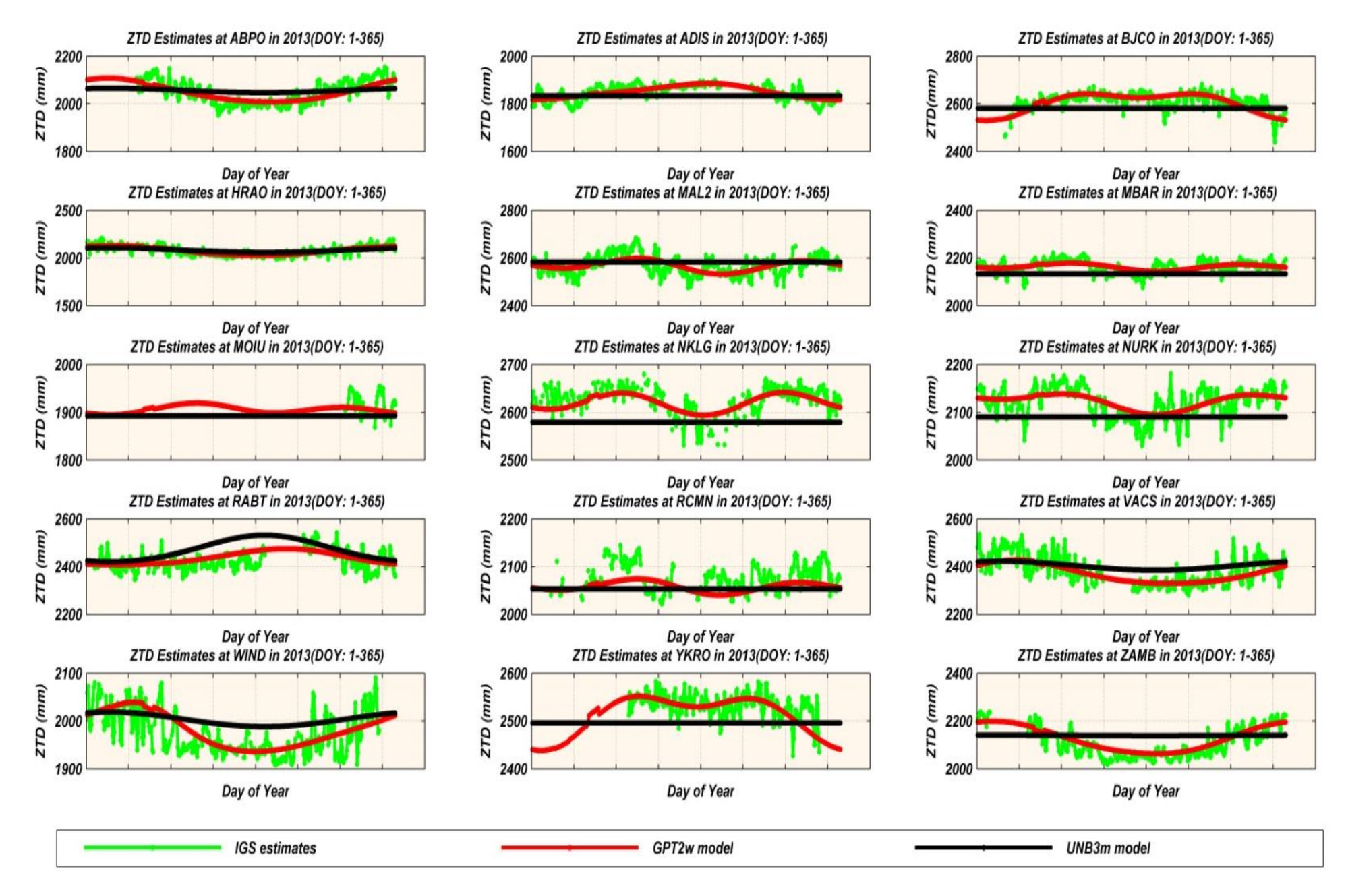


Figure 2: Time series plot of the UnB3m, GPT2w, and IGS estimation of ZTD for 2013

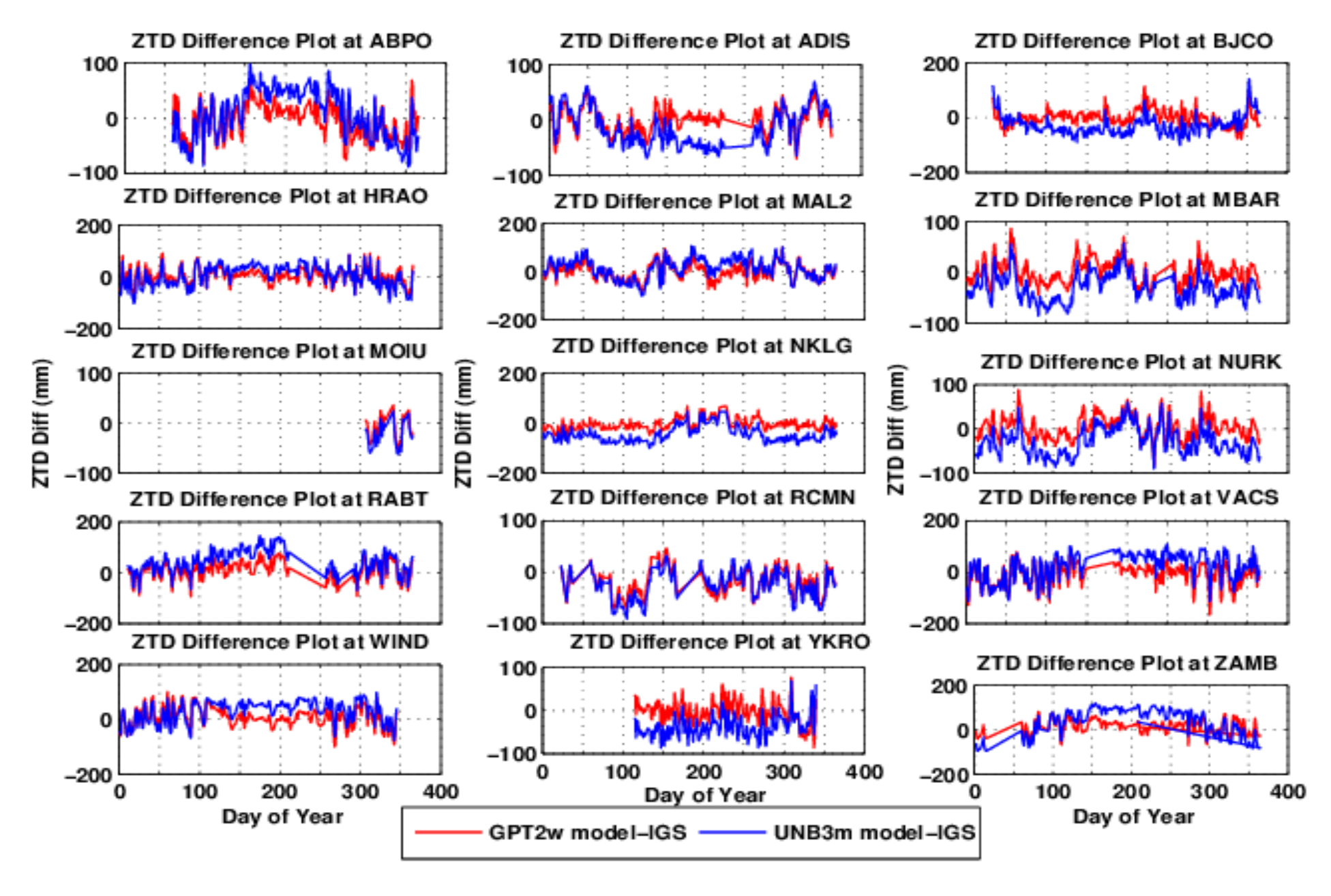


Figure 3(a): Time series plot of the difference of UnB3m and GPT2w models to IGS estimation of ZTD for 2013

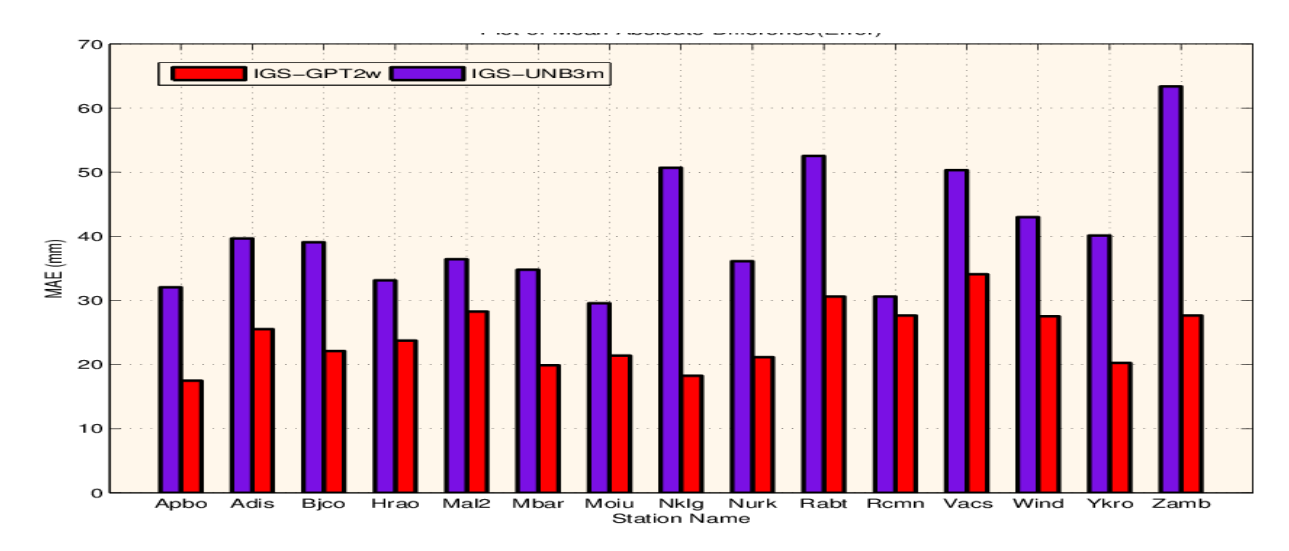


Figure 3(b): Plot of the Mean Absolute difference (errors) for the different stations

A fundamental input parameter in the estimation of ZTD from the UNB3m and GPT2w model is the station elevation. It is therefore important to identify the dependence of the ZTD estimates on elevation and also the effect of the individual station elevation and their corresponding RMSE as contained in Table 4. The correlation coefficient (r) was employed to ascertain the linear inter-relationship among the IGS product, UNB3m, GPT2w, and station elevation. The resultant correlation matrix is presented in Table 5.

Table 5: Correlation matrix of the IGS product, UNB3m, GPT2w, and station elevation

	Elevation	IGS	GPT2W	UNB3m
Elevation	1	-0.9800	-0.9825	-0.9942
IGS	-0.9800	1	0.9995	0.9939
GPT2w	-0.9825	0.9995	1	0.9953
UNB3m	-0.9942	0.9939	0.9953	1

From Table 5 it is clear that the ZTD estimates from the models under investigation exhibit a very strong negative correlation. Thus, an increase in station elevation results in corresponding decrease in the amount of ZTD over the station. This is further confirmed from Figure 4, that the best line of fit for the IGS, UNB3m and GPT2w when plotted against the corresponding station elevation has a negative gradient, indicating the inverse proportional relationship by all three models under investigation.

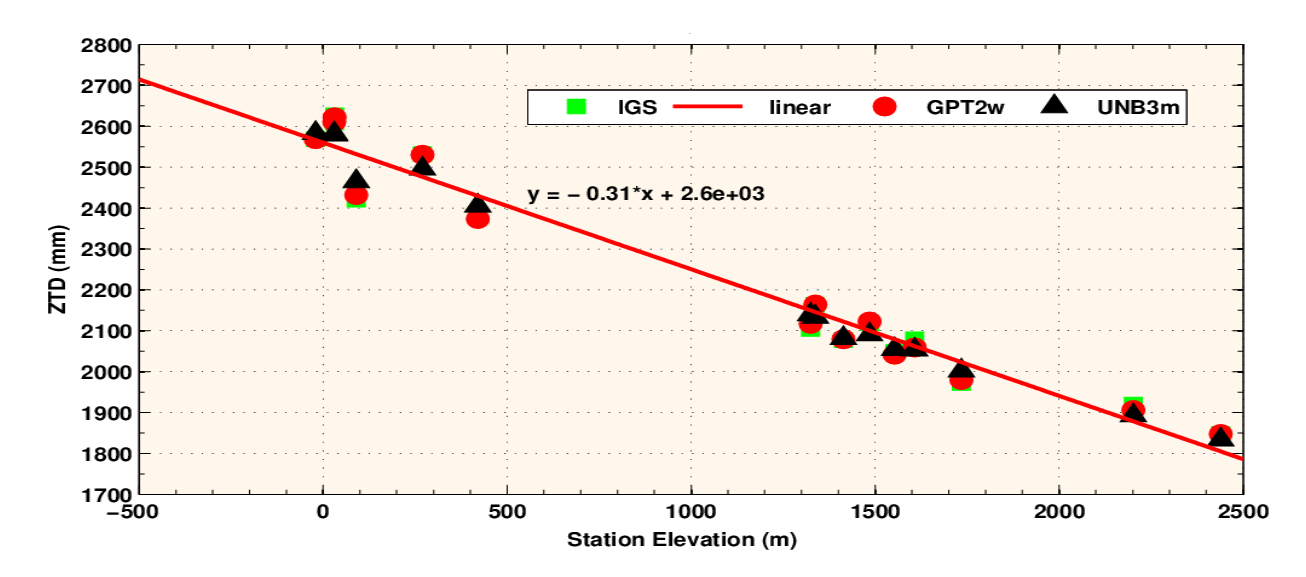


Figure 4: Plot of mean ZTD estimates against station elevation

Furthermore, the RMSE of the different stations as presented earlier in Table 4 were plotted against the station elevation to ascertain the influence of the latter on the corresponding RMSE. From Figure 5 it is evident that no relationship exists between the RMSE and station elevation, which implies that the station elevation does not influence the magnitude of error in ZTD estimates from the UNB3m and GPT2w models. It is again observed in Figure 5 that the RMSE for the GPT2w model was smaller at all height values than those of the UNB3m model.

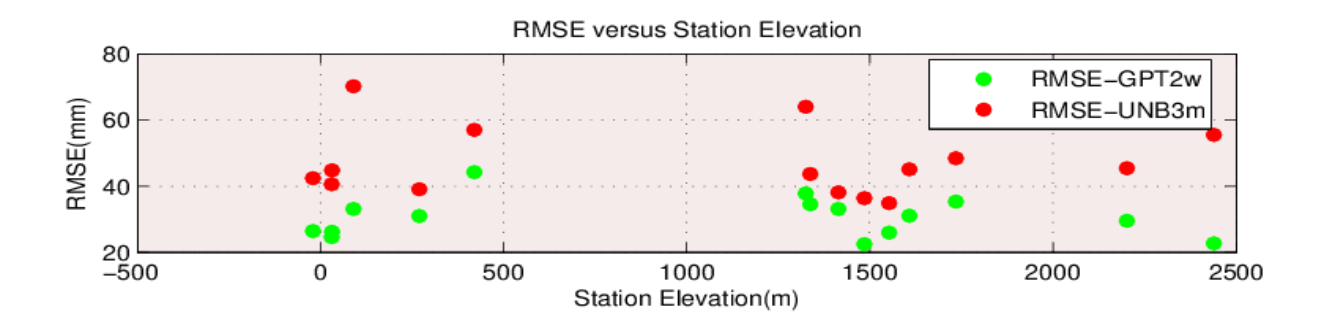


Figure 5: Plot of RMSE versus station elevation

The latitudinal dependence of the models was also investigated by comparing the station latitude with the corresponding RMSE and MEF values as shown in Figures 6 and 7. In Figure 6, it is indicative that both the UNB3m and GPT2w models perform better at low latitude ranges, i.e., from $1^{\circ} - 10^{\circ}$. Again, the GPT2w performs better at all latitudes.

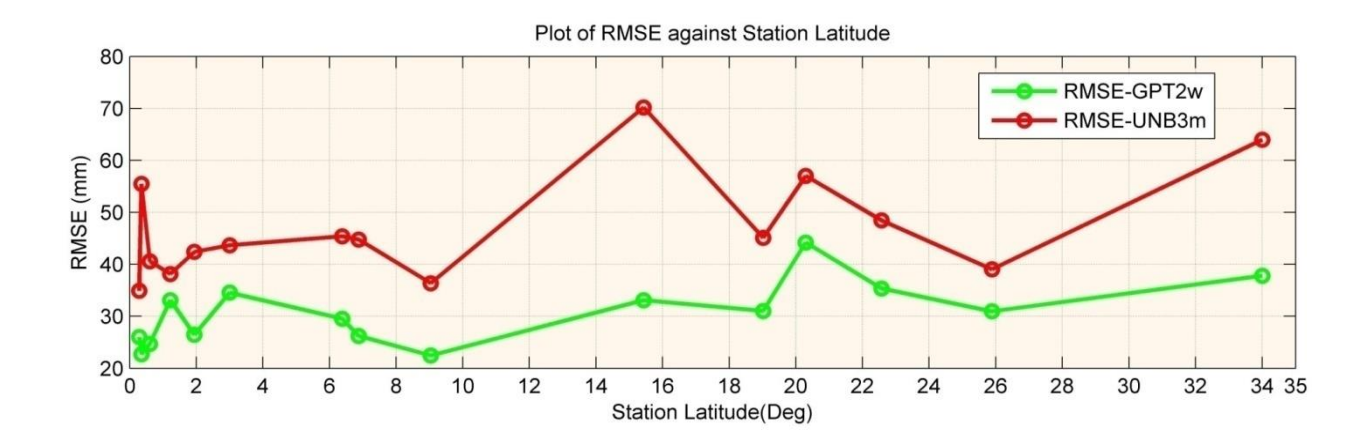


Figure 6: Plot of RMSE versus station absolute latitude

As seen in Figure 7, the MEF value for the GPT2w appears to be small at low latitudes range of $0^{\circ} - 2^{\circ}$, at the same latitude range the UNB3m model is seen to agree with the GPT2w model. Again, the GPT2w have better MEF values for all of the station latitude ranges, except at the stations situated almost at the equator (MBAR, NKLG, and NURK).

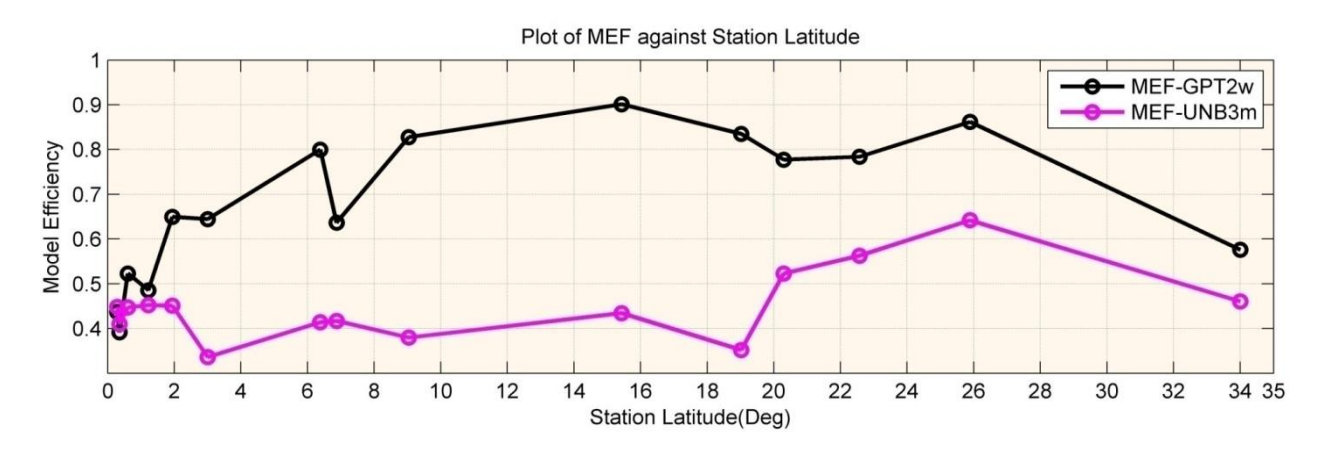


Figure 7: Plot of MEF versus station absolute latitude

Figures 8 and 9 are the ZTD, ZHD and ZWD time series of HRAO for the month of January 2013. HRAO is one the few IGS stations on the continent of Africa that is collocated with meteorological sensors as identified by Isiove et al., 2015. The station is equipped with **MET** 4 meteorological system and data downloaded a was at ftp://cddis.gsfc.nasa.gov/pub/gps/data/daily/. This is a highly accurate meteorological measurement system for GNSS meteorology and environmental monitoring; it measures pressure with an accuracy of +/- 0.05hpa from 500 to 1100hpa, temperature +/- 0.2deg Celsius, and humidity +/- 2% to 100% at standard temperature.

In Figure 8, ZTD was computed with the Saastamoinen formula using measured pressure and temperature at the site and was compared with the IGS product, UNB3m and

GPT2w models. The corresponding ZHD and ZWD are according to Equations 1 and 3. From Figure 8 it is indicative that the ZTD trend from the Saastamoinen model agrees very well with the IGS solution, with the GPT2w showing very little variation from the IGS solution, and the UNB3m appearing almost constant throughout. The ZHD from IGS product was retrieved from the measured pressure values at the station with the Saastamoinen formula. It can be seen that there is strong agreement among the IGS, Saastamoinen and GPT2w models, this can be interpreted as an indication of the effectiveness of the GPT2w models, and the UNB3m model could still not account for the variation in daily ZHD at the station. Looking at the ZWD estimates, there is again very strong agreement between the Saastamoinen and IGS product. The UNB3m and GPT2w models show weakness in accounting for the daily variation in ZWD estimation, though a careful scrutiny of the data reveal insignificant variations in the ZWD values for the GPT2w model.

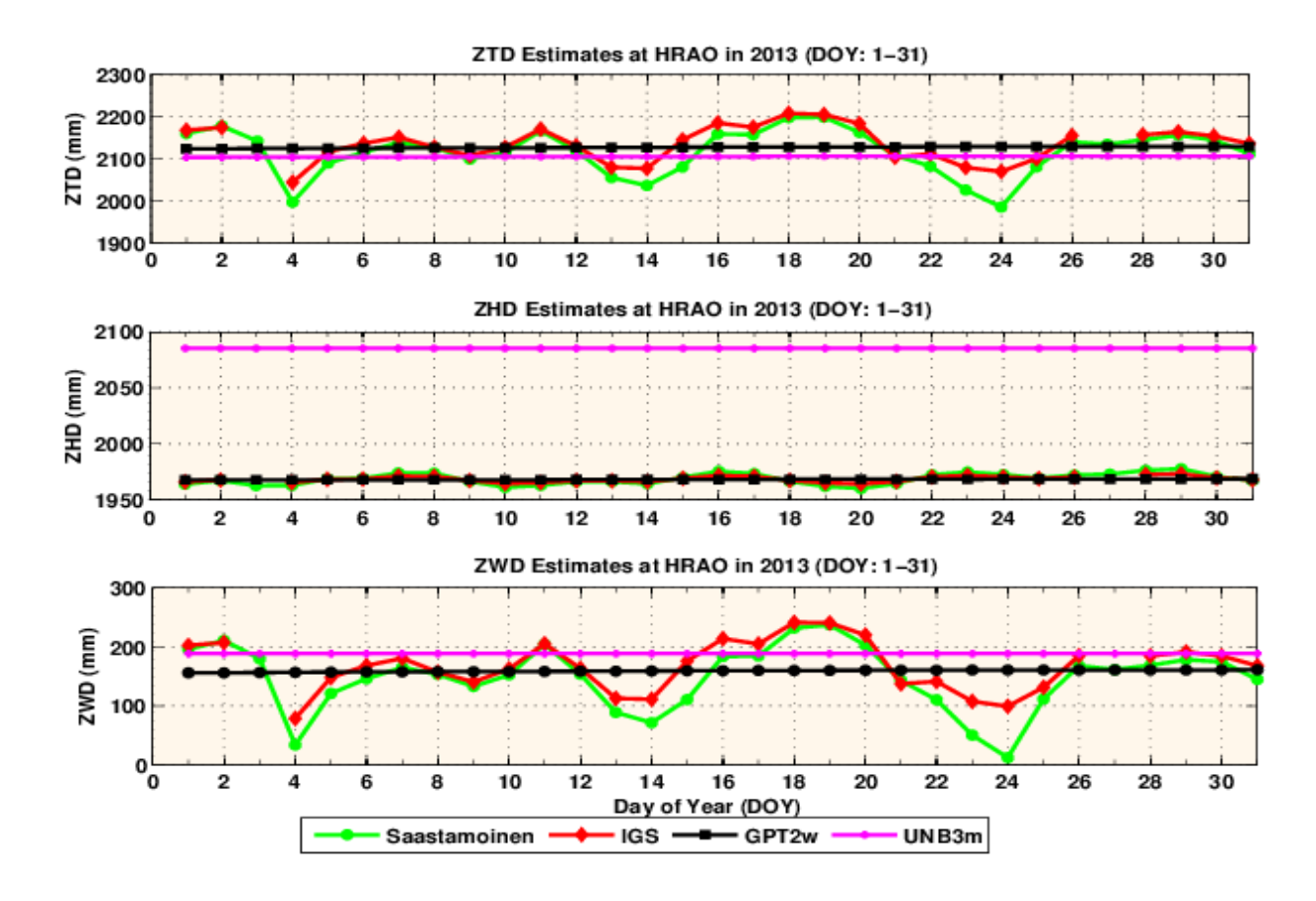


Figure 8: Estimated ZTD, ZHD, and ZWD from the Saastamoinen formula, IGS product, GPT2w model, and UNB3m model at HRAO for doy of Year 1-31, 2013. The Saastamoinen formula using meteorological parameters measured with a MET 4A unit for ZHD and ZWD estimation, the ZHD from the IGS product was also retrieved utilizing the measured parameter from the Met 4A unit

Figure 9 presents some very contrasting results, ZTD was computed with the Saastamoinen formula using standard pressure and temperature values at the site and was compared with the IGS product, UNB3m and GPT2w models. The corresponding ZHD and ZWD from the Saastamoinen formula are according to Equations 1 and 3. From Figure 9 it is clear that the Saastamoinen formula fails to agree with the other methods, with the GPT2w and the UNB3m models appear almost constant throughout. The ZHD from IGS product was retrieved from the standard pressure values at the station with the Saastamoinen formula. It can be seen that there is strong agreement between the IGS estimates, and GPT2w model, thus this is another indication of the effectiveness of the GPT2w model, both the UNB3m and Saastamoinen formula could still not account for the variation in daily ZHD at the station and the Saastamoinen formula appears to overestimate the quantity. Looking at the ZWD estimates, there is very strong agreement between the Saastamoinen formula and the GPT2w model. Careful inspection of the data reveals small variations in the ZWD values for the GPT2w model. Again the UNB3m model shows weakness in accounting for the daily variation in ZWD estimation.

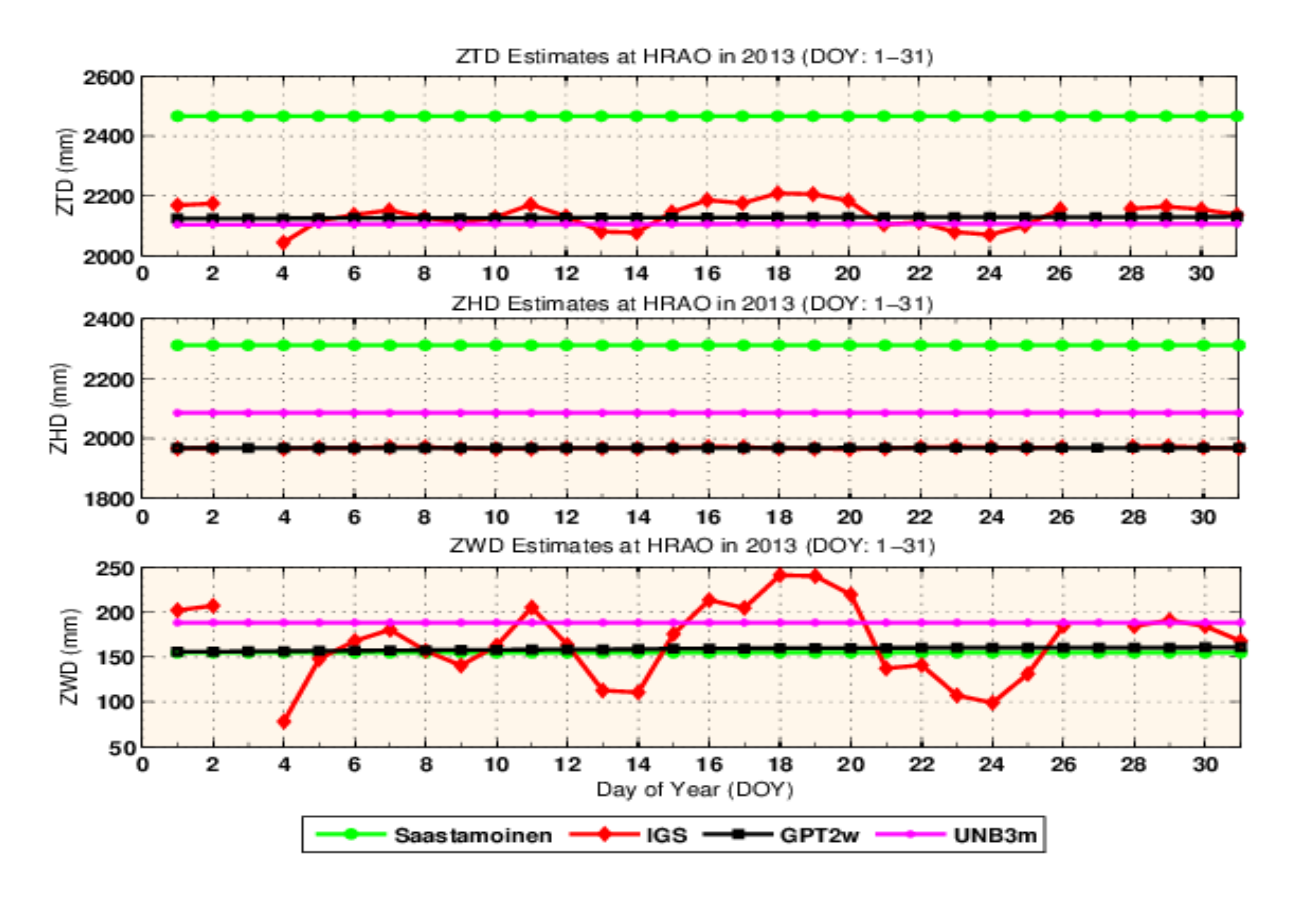


Figure 9: Estimated ZTD, ZHD, and ZWD from the Saastamoinen formula, IGS product, GPT2w model, and UNB3m model of HRAO for doy of Year 1-31, 2013. The Saastamoinen

formula using standard meteorological parameters for ZHD and ZWD estimation, the ZHD from the IGS product was also retrieved utilizing standard met parameters

4.0 Concluding Remarks

We have estimated the accuracies of the UNB3m and GPT2w tropospheric correction models over Africa by using the ZTD time series from the global IGS GNSS network in Africa, and Saastamoinen formula based on measured meteorological parameters. The UNB3m and GPT2w models are unique representations of the two distinct groups of blind tropospheric models in global use. The UNB3m model utilises a lookup table with annual mean and amplitude of temperature, pressure, and water vapour pressure varying with regard to latitude and height. These parameters are computed for a particular latitude and day of the year using a cosine function of the annual variation and a linear interpolation for latitude. Similarly, the GPT2w is based on gridded values of water vapour pressure, water vapour decrease factor, and weighted mean temperature. All climatological parameters have been derived consistently from monthly mean pressure level data of ERA-Interim fields with a horizontal resolution of 1°. Thus, based on the comparisons we arrive at the following conclusions:

- I. The accuracy of ZTD correction from the GPT2w model is well within the range of 50 mm, and this accuracy can meet the needs of the tropospheric delay correction of the order of meters, in GNSS positioning.
- II. Both models perform well at the low equatorial region of Africa and respond to station elevation in the similar fashion.
- III. The GPT2w represents an excellent model for ZHD estimation due to its high accurate pressure estimates.
- IV. The GPT2w model shows very good signatures of seasonal ZTD trend but weak daily variations, but in both cases better than the UNB3m model.
- V. The Saastamoinen model performs poorly with the use of standard atmospheric parameters and thus fails to address the peculiarities of the African GNSS network which is characterized by a lack of sensors for measuring meteorological data. Thus, better estimates of ZTD from GNSS can be obtained with the GPT2w model without actual field measurements.

Finally, there was better agreement between the GPT2w and IGS estimate at all stations. Therefore, the GPT2w model can be used as a correction model of the tropospheric error for the GNSS real-time positioning and navigation on the African Continent.

Conflict of Interests

The authors declare that there is no conflict of interests regarding the publication of this paper.

Acknowledgement

This study was supported by HartRAO and funded by the University of Pretoria PhD Research Support grant to the first author. The authors would like to express their profound gratitude to the numerous reviewers for their constructive comments that helped to improve the manuscript.

References

Askne, J and Nordius, H 1987, 'Estimation of tropospheric delay for microwaves from surface weather data', *Radio Science*, 22(3), pp. 379-386.

Berman, AL 1976, *The Prediction of Zenith Range Refraction From Surface Measurements of Meteorological Parameters*, Jet Propulsion Laboratory, California Institute of Technology, Pasadena, California, 15 July, National Aeronautics and Space Administration Technical Report 32–1602, pp. 40.

Black, HD and Eisner, A 1984, 'Correcting satellite doppler data for tropospheric effects', *J. Geophys. Res.*, 89, D2, 2616-2626.

Boehm, J Möller, G Schindelegger, M Pain, G and Weber, R 2014, 'Development of an improved blind model for slant delays in the troposphere (GPT2w)', *GPS Solutions*, doi: 10.1007/s10291-014-0403-7.

Boehm, J Heinkelmann, R and Schuh, H 2007, 'Short Note: A Global Model of Pressure and Temperature for Geodetic Applications', *Journal of Geodesy*, 81 (10), pp. 679-683, doi: 10.1007/s00190-007-0135-3.

Boehm, J Niell, A Tregoning, P and Schuh, H 2006b, 'Global Mapping Function (GMF): A new empirical mapping function based on data from numerical weather model data', *Geophysical Research Letters*, 33, L07304, doi: 10.1029/2005GL025546.

Boehm, J Werl, B and Schuh, H 2006a, 'Troposphere mapping functions for GPS and very long baseline interferometry from European Centre for Medium-Range Weather Forecasts operational analysis data', J. Geophys. Res., 111, B02406.

Byun, SH and Bar-Sever, YE 2009, 'A New type of Troposphere Zenith Path Delay Product of the International GNSS Service', *J. Geod.*, 83(3-4), pp.1-7.

COESA 1966, 'U.S. Standard Atmosphere Supplements, 1966', U.S. Committee on Extension to the Standard Atmosphere. Sponsored by Environmental Science Services Administration, National Aeronautics and Space Administration, United States Air Force and published by the Superintendent of Documents, U.S. Government Printing Office, Washington, D.C.

Collins, JP and Langley, RB 1997, A Tropospheric Delay Model for the User of the Wide Area Augmentation System. Final contract report for Nav Canada, Department of Geodesy and Geomatics Engineering Technical Report No. 187, University of New Brunswick, Fredericton, N.B., Canada.

Collins, JP and Langley, RB 1998, 'The Residual Tropospheric Propagation Delay: How Bad Can It Get?', *Proceedings of ION GPS-98, 11th International Technical Meeting of the Satellite Division of The Institute of Navigation*, Nashville, TN, 15-18 September 1998, pp. 729-738.

Collins, JP and Langley, RB 1999, Nominal and Extreme Error Performance of the UNB3 Tropospheric Delay Model, Final contract report for Nav Canada, Department of Geodesy and Geomatics Engineering, Technical Report No. 204, University of New Brunswick, Fredericton, N.B., Canada.

Davis, JL Herring, TA Shapiro, *I Rogers, AE and Elgered, G 1985, 'Geodesy by interferometry: Effects of* atmospheric modelling errors on estimates of base line length', *Radio Sci.*, 20, pp.1593–1607.

Dodo, JD and Idowu, TO 2010, 'Regional Assessment of the GPS Tropospheric Delay Models on the African GNSS Network', *Journal of Emerging Trends in Engineering and Applied Sciences (JETEAS)* 1(1), pp. 113-121.

Dodson, AH Chen, W Baker, HC Penna, NT Roberts, GW Westbrook, J and Jeans R 1999, 'Assessment of EGNOS Tropospheric Correction Model', *Proceedings of ION GPS-99, 12th International Technical Meeting of the Satellite Division of The Institute of Navigation*, Nashville, TN, 14-17 September 1999, pp. 1401-1407.

ESA Galileo Programme 2012, Galileo Reference Troposphere Model for the user receiver, ESA-APPNG-REF/00621-AM, ver. 2.7.

Essen, L and Froome, KD 1951, 'The refractive indices and dielectric constants of air and its principal constituents at 24,000 Mc/s', *Proc. Phys. Soc.* B., 64, 10, 862-875, http://iopscience.iop.org/0370-1301/64/10/303.

Farah, A 2011, 'Assessment of UNB3M neutral atmosphere model and EGNOS model for near equatorial tropospheric delay correction', *Journal of Geomatics*, 5, no.2, pp.67-72.

Hopfield, H.S., 1969, 'Two Quartic Tropospheric refractive profile for correcting satellite data', *J. Geophys. Res.*, 74(18), 4487-4499.

Ifadis, II 1986, *The Atmospheric delay of radio waves: Modeling the elevation dependence on a global scale*, Technical Report 38L. Chalmers University of Technology, Goteborg, Sweden.

Isioye, OA Combrinck, L Botai, JO and Munghemezulu, C 2015, 'The Potential of Observing African Weather with GNSS Remote Sensing', *Advances in Meteorology*, Volume 2015, Article ID 723071, http://dx.doi.org/10/1155/2015/723071.

Lagler, K Schindelegger, M Böhm, J Krásná, H and Nilsson, T 2013, 'GPT2: Empirical slant delay model for radio space geodetic techniques', *Geophys. Res. Lett.*, 40, pp. 1069–1073, doi:10.1002/grl.50288.

Leandro, RF Santos, MC and Langley, RB 2006, *UNB Neural Atmosphere Models: Development and Performance*. Proceedings of ION NTM 2006, pp. 564-573, Monterey, California, USA.

Leggett, RW and Williams, LR 1981, 'A reliability index for models', *Ecological Modelling*, (13), pp. 303-312.

McCarthy, DD and Petit, G 2004, IERS *Conventions* (2003). IERS Technical Note 32, Verlag des undesamts für Kartographie und Geodäsie, Frankfurt am Main.

Moller, G Weber, R Boehm, J 2013, 'Improved Troposphere Blind Models based on Numerical Weather Data', *In the Proceedings of the 26th International Technical Meeting of the ION satellite Division*, ION GNSS + 2013, Nashville, Tennessee, September 16-20, 2013.

Murphy, AH 1988, 'Skill scores based on the mean square error and their relationship to the correlation coefficient', *Mon. Weather Rev.*, 116, pp. 2417-2424.

Niell, AE 1996, 'Global mapping functions for the atmosphere delay at radio wavelengths', *Journal of Geophysical Research*, 101,(B2), pp. 3227-3246.

Orliac, E 2002, *Troposphere Delay Models for Satellite Navigation Applications*. Diploma thesis, École Polytechnique Fédérale de Lausanne, Lausanne, Switzerland.

Penna, N Dodson, A and Chen, W 2001, 'Assessment of EGNOS Tropospheric Correction Model', *Journal of Navigation*, 54, (1), pp. 37-55.

RTCA, Inc. 2001 DO-229C, Minimum Operational Performance Standards for Global Positioning System/Wide Area Augmentation System Airborne Equipment, SC-169, RTCA, Inc., Washington, D.C.

Saastamoinen, J 1972, Atmospheric correction for the troposphere and the stratosphere in radio ranging satellites, in 'The use of artificial satellites for geodesy', *Geophys. Monogr. Ser.* pp. 247-251, AGU, Washington.

Schingelegger, M Moller, G Boehm, J Weber, R and Pain, G 2014, *Troposphere Delay Models in Blind Mode: Towards Improved Predictions of the Wet Component*, EGU General Assembly, Vienna, 27 April- 2 May 2014.

Shcherbakov, MV Brebels, A Shcherbakova, NL Tyukov, AP Janovsky, TA Kamaev, VA 2013, 'A survey of forecast error measures', *World Applied Sciences Journal*, 24, pp. 171-176, doi:10.5829/idosi.wasj.2013.24.itimes.80032.

Tuka, A and El-Mowafy, A 2013, 'Performance Evaluation of different Troposphere Delay Models and Mapping Functions', *Measurement* 46(2013), pp. 928-937, http://dx.doi.org/10.1016/j.measurement.2012.10.015

Won, J Park, K-D Ha, J and Cho, J 2010, Effects of tropospheric mapping functions on GPS data processing, *J. Aston .Space Sci.*, 27(1), 21-30, doi: 10.5140/JASS.2010.27.1.021.

Zus, F Dick, G Dousa, J and Wickert, J 2015, 'Systematic errors of mapping functions which are based on the VMF1 concept', *GPS Solutions*, 19(2), 277-286, doi: 10.1007/s10291-014-0386-4.